Neutron and Gamma-ray Emission Double Differential Cross Sections for the Nuclear Reaction by 1.5 GeV π^+ Incidence

Kiminori IGA[*1], Kenji ISHIBASHI[*1], Nobuhiro SHIGYO[*1], Naruhiro MATSUFUJI[*1,+1],
Tatsushi NAKAMOTO[*1,+2], Keisuke MAEHATA[*1], Masaharu NUMAJIRI[*2],
Shin-ichirou MEIGO[*3], Hiroshi TAKADA[*3], Satoshi CHIBA[*3],
Takashi NAKAMURA[*4], and Yukinobu WATANABE[*5]

*1 *Department of Nuclear Engineering, Kyushu University, Hakozaki, Higashi-ku, Fukuoka-shi 812-81.*
*2 *High Energy Accelerator Research Organization, Oho, Tsukuba-shi 305.*
*3 *Japan Atomic Energy Research Institute, Tokai-mura, Ibaraki-ken 319-11.*
*4 *Cyclotron-RI Center, Tohoku University, Aramaki, Aoba-ku, Sendai-shi 980-77.*
*5 *Energy Conversion Engineering, Kyushu University, Kasuga-koen, Kasuga-shi 816.*
Present address
+1 *National Institute of Radiological Sciences, Anagawa, Inage-ku, Chiba 263.*
+2 *High Energy Accelerator Research Organization, Oho, Tsukuba-shi 305.*
e-mail: iga@kune2a.nucl.kyushu-u.ac.jp

Neutron and gamma-ray production double differential cross sections were measured for iron by the use of 1.5 GeV π^+ mesons. The measured cross sections were compared with the calculated values by HETC-KFA2. For the neutrons, the calculated results deviate from the experimental data in the neutron energy region below 30 MeV. The calculated values of gamma-ray production agree with the experimental data at gamma-ray energies from 1 to 7 MeV within a factor of three.

I. INTRODUCTION

The proton incident spallation reaction has been investigated for such application as spallation neutron source and accelerator-driven transmutation system. Nuclear data at energies around GeV are necessary for designing such systems. Especially, the neutron production cross sections are important. We measured double differential cross sections on production of spallation neutrons before [1, 2]. However, neutron production cross sections by pion incidence are also important, because the secondary pions which are made by the proton-nucleus reaction produce neutrons. Gamma-ray production cross sections are required of researches on shielding of these systems. The neutron and gamma-ray production cross sections by pion incidece, however, have not been taken so far. In this study, we present neutron and gamma-ray production double cross sections by 1.5 GeV π^+ mesons incident on iron. The experimental data are compared with the results calculated by HETC-KFA2 [3].

II. EXPERIMENT AND DATA ANALYSIS

The experiment was carried out at the $\pi2$ beam line of the 12 GeV proton synchrotron at National Laboratory for High Energy Physics (at present, High Energy Accelerator Research Organization). The experimental method was written in Refs. [1], [2], and [4] and described briefly here. Protons with energies around GeV produces pions having energies of several hundred MeV, but we chose an incident π^+ energy of 1.5 GeV for ease of performing the experiment.

An iron target 4.9 cm in diameter and 3.0 cm thick was located at the beam line height of 1.7 m. The experimental arrangement is illustrated in Fig. 1. Tow different sizes of NE213 detectors were placed at directions of 30, 90 and 150 deg relative to the beam. The larger NE213 detectors 12.7 cm in diameter and 12.7 cm thick were placed at a distance of 1 m from a target, while the smaller NE213 detectors 5.08 cm in diameter and 5.08 cm thick were put at a distance of 0.6 m. The scintillators were used for simultaneous measurement of neutrons and prompt gamma-rays. The time-of-flight (TOF) and photomultiplier-charge data were taken. All data were analyzed with an off-line method.

In the experiment, both target-in and -out measurements were performed. Fig. 2 shows an example of TOF spectra in the target-in and -out measurements. The target-in spectra have a broad peak at a time of 30 ns. Target-out results gives flash gamma-rays, which were produced by upstream plastic scintillators, and slightly prior to those emitted from the target in the target-in measurement. Neutron and gamma-ray spectra were obtained by subtracting the results of the target-out measurement from those of the target-in. Neutron spectra were separated from gamma-ray ones by the pulse-shape discrimination based on a two-gate integration method [5]. The discrimination results are shown in Fig. 3.

The neutron energy was determined by the TOF measurement. The neutron TOF spectrum is plotted in Fig. 4. The flash gamma-ray peak was taken as the time reference for the neutron TOF. The broad peak indicates neutrons from the evaporation process. The neutron detection efficiencies were obtained from calculation results of SCINFUL [6] and SECIL [7] codes. The results of SCINFUL were utilized for neutron detection efficiencies below 80 MeV. The results of CECIL were adjusted to smoothly connect with those of SCINFUL at 80 MeV and were employed above 80 MeV.

The data analysis of gamma-ray was restricted to the prompt gamma-ray production. A TOF time window of 2.8 ns on both sides of prompt gamma-peak was chosen. A charge sensitive Analog-to-Digital Converter spectrum of gamma-rays is shown in Fig. 5. The counts of gamma-ray event decrease rapidly with increasing ADC channel. The gamma-ray energy calibration of the charge spectra was made by the use of checking sources of ^{137}Cs and ^{60}Co, and 4.4 MeV gamma-ray from interaction of Am-Be source neutrons with C. Measured charge spectra were unfolded to obtain gamma-ray emission spectra. Unfolding was carried out by a FERDo-U [8] code. The response function and gamma-ray detection efficiencies of NE213 were calculated by an EGS4 [9] code.

A correction for the effect of multiple-scattering in the target was required for the data analysis because the target thickness of 3.0 cm was not so thin. The effects of multiple-scattering neutrons and gamma-rays were quantitatively checked by the calculation with combination of NMTC/JAERI [10] and MCNP4A [11] codes. The MCNP4A code was adopted to take into consideration the interaction of secondary neutrons and gamma-rays below 20 MeV. The cross section obtained for the ideal thin target was divided by the apparent cross section calculated for the actual thick target. In addition, the effect of gamma-ray attenuation was corrected by using the EGS4 code.

III.   RESULTS AND DISCUSSION

The measured and computed results are shown in Figs. 6 and 7. In Fig. 6, the dashed lines show the calculation results of the standard HETC code which employs the free nucleon-nucleon (NN) collision cross sections in the cascade process. The dashed lines generally reproduce the experiment in the neutron energy region from 30 to 200 MeV. In contrast, the calculations overestimate the cross sections below 30 MeV. Solid lines indicate the computation results by the HETC code with modified NN collision cross sections presented by Li and Machleidt [12, 13]. They

took account of the in-medium effect for NN elastic scattering in target nuclei. The solid lines are lower than the dashed ones at energies below 30 MeV, and closer to the experimental data. Adoption of the in-medium NN cross sections increases the mean free path of nucleons, so that it enhances the neutron emission from the cascade process in the high energy region roughly above 100 MeV. The enhancement of nucleon emission in the cascade process decreases the excitation energy of remnant nucleuses and suppresses the neutron emission from the evaporation process.

In Fig. 7, the solid lines show the calculation results of HETC-KFA2. These lines agree with the experimental data in the gamma-ray energy region from 1 to 7 MeV within a factor of three. Cross marks present calculated cross sections of the gamma-ray production from the π^0 decay, and dashed lines show the influence of the gamma-rays. The π^0 decay gamma-rays were mistreated in the unfolding, because the response function for gamma-rays above 60 MeV has no clear peak and is almost independent of the incident energy. The influence of π^0 decay gamma-rays was obtained in Monte Carlo simulation. The cross sections in the energy range above 20 MeV were mainly ascribed to the mistreated events, since they were comparable to the evaluated influence of the π^0 decay gamma-rays.

IV. CONCLUSION

The neutron and gamma-ray production double differential cross sections were measured for 1.5 GeV π^+ mesons incident on the iron target. For the neutron production cross sections, the experimental data are not reproduced by the standard HETC code particularly at the neutron energies below 30 MeV. The adoption of in-medium NN cross sections leading to the larger mean free path improves the agreement between the calculations and the experiments. For gamma-ray results, the calculation results agree with the experimental ones in the gamma-ray energy region from 1 to 7 MeV within a factor of three.

**REFERENCES**

[1] Nakamoto, T., *et al.*: *J. Nucl. Sci. Technol.*, **32**, 827 (1995).

[2] Ishibashi, K., *et al.*: *J. Nucl. Sci. Technol.*, **34**, 529 (1997).

[3] Cloth, P., *et al.*: HERMES, High Energy Radiation Monte Carlo Elaborate System, *KFA-IRE-E.* AN/12/88 (1988).

[4] Nakamoto, T., *et al.*: *J. Nucl. Sci. Technol.*, **34**, 860 (1997).

[5] Zucker, M. S. and Tsoupas, N.: *Nucl. Instrum. Methods*, **A299**, 281 (1990).

[6] Dickens, J. K.: *ORNL*-6452 (1988).

[7] Cecil, R. A., *et al.*: *Nucl. Instrum. Methods*, **161**, 439 (1979).

[8] Burrus, W. R., :*ORNL-Report*-3743 (1995).

[9] Nelson, W. R., *et al.*: *SLAC-Report*-265 (1995).

[10] Nakahara, Y., *et al.*: *JAERI-M* 82-198 (1982).

[11] Briesmeister, J. F., *et al.*: *LA*-12625 (1993).

[12] Li, G. Q. and Machleidt, R.: *Phys. Rev.*, **C48**, 1702 (1993).

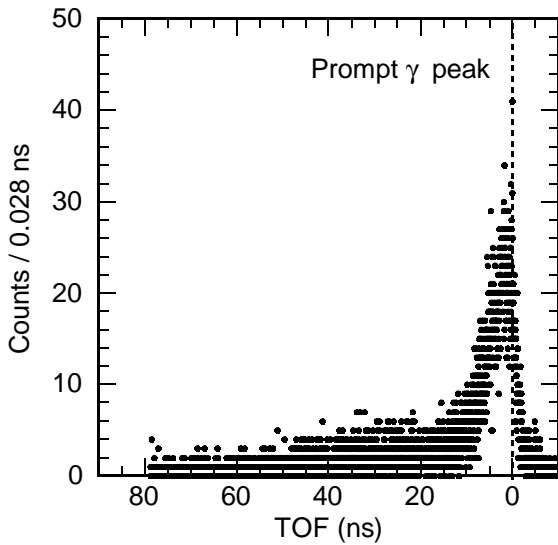[13] Li, G. Q. and Machleidt, R.: *Phys. Rev.*, **C49**, 566 (1994).
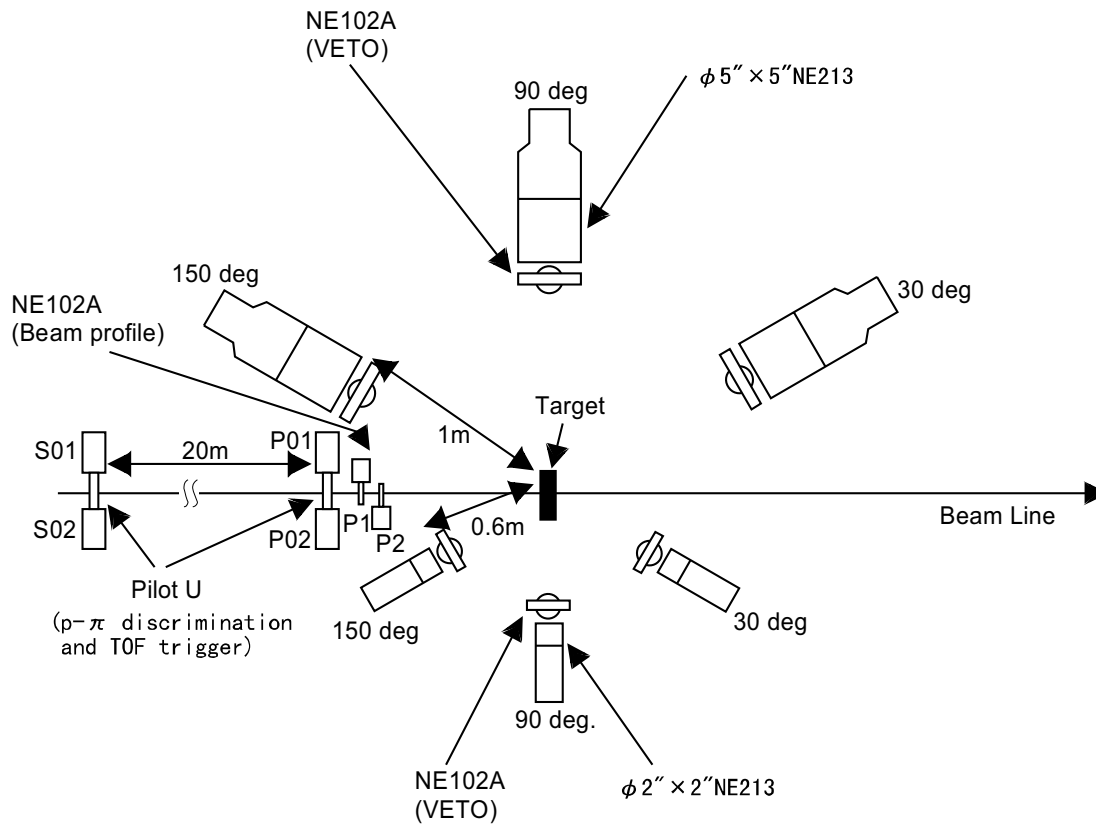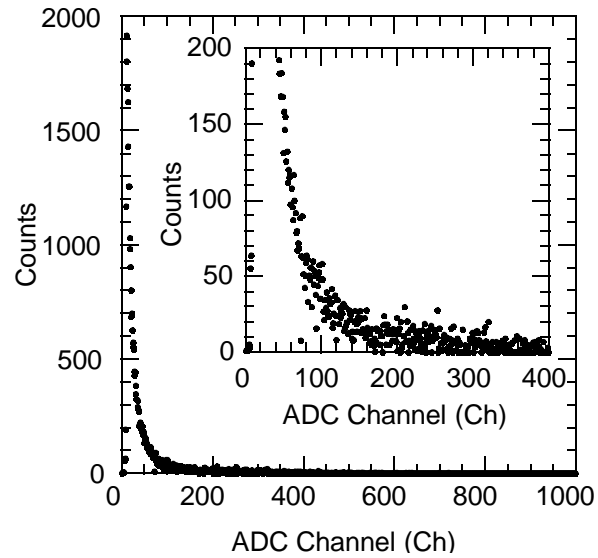
Fig. 1 Illustration of experiment arrangement.
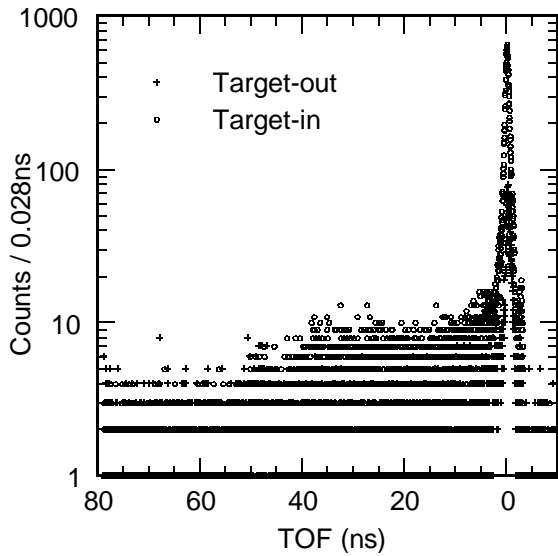
Fig. 2 TOF spectra of the target-in and -out measurements with the 12.7 (dia.) × 12.7 (thick) cm NE213 at 30 deg. The spectra includes both neutron and gamma-rays.
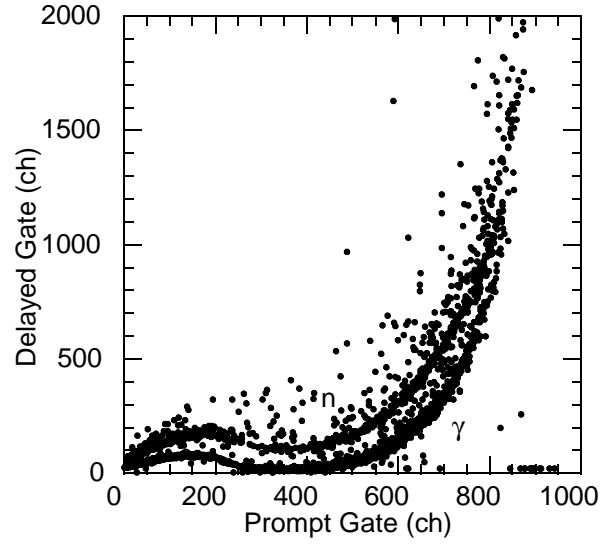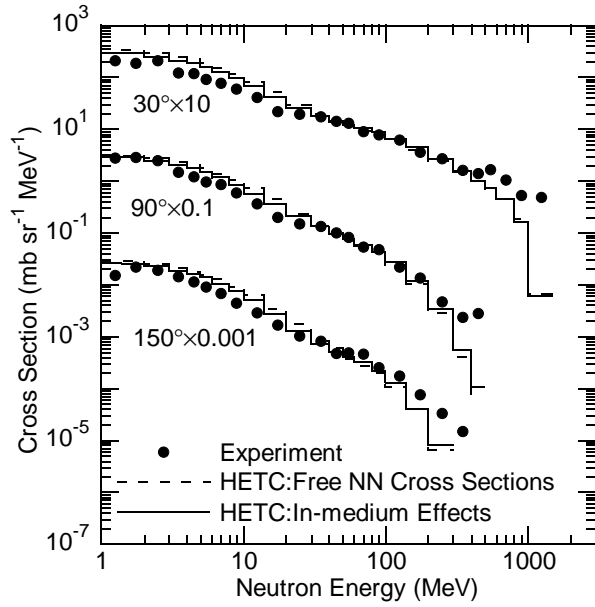

Fig. 3 Neutron and gamma-ray pulse-shape discrimination by two-gate integration method.


Fig. 4 TOF spectra of neutrons measured with the 12.7 (dia.) × 12.7 (thick) cm NE213 at 30 deg.

Fig. 5 Charge sensitive ADC spectrum of gamma-ray measured with the 12.7 (dia.) × 12.7 (thick) cm NE213 at 30 deg. The inset is displayed in a magnified scale.

Fig. 6 Neutron production double differential cross sections for 1.5 GeV π^+ on Fe. Dots show the experimental results. Dashed and solid lines show the HETC results with NN cross sections in the free space and in nuclear medium, respectively.
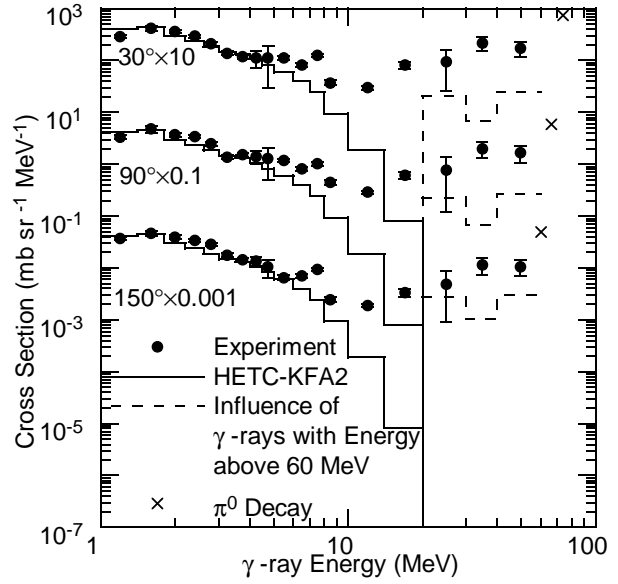
Fig. 7 Unfolded results on gamma-ray production double differential cross sections for 1.5 GeV π^+ on Fe. Dots show the experimental results. Solid lines indicate calculation results by HETC-KFA2. Cross marks present calculated cross sections of the gamma-ray production from the π^0 decay, and dashed lines show the influence of the π^0 gamma-rays.